Available online at www.sciencedirect.com
SCIENCE DIRECT®
Biochemical and Biophysical Research Communications 338 (2005) 191–197
BBRC
www.elsevier.com/locate/ybbrc

Kinetic and spectroscopic investigation of Co^{II}, Ni^{II}, and *N*-oxalylglycine inhibition of the Fe^{II}/α-ketoglutarate dioxygenase, TauD

Efthalia Kalliri [a], Piotr K. Grzyska [b], Robert P. Hausinger [b,c,*]

[a] *Department of Chemistry, Michigan State University, East Lansing, MI 48824, USA*
[b] *Department of Microbiology and Molecular Genetics, Michigan State University, East Lansing, MI 48824, USA*
[c] *Department of Biochemistry and Molecular Biology, Michigan State University, East Lansing, MI 48824, USA*

Received 13 July 2005
Available online 8 September 2005

Abstract

Co^{II}, Ni^{II}, and *N*-oxalylglycine (NOG) are well-known inhibitors of Fe^{II}/α-ketoglutarate (αKG)-dependent hydroxylases, but few studies describe their kinetics and no spectroscopic investigations have been reported. Using taurine/αKG dioxygenase (TauD) as a paradigm for this enzyme family, time-dependent inhibition assays showed that Co^{II} and Ni^{II} follow slow-binding inhibition kinetics. Whereas Ni^{II}-substituted TauD was non-chromophoric, spectroscopic studies of the Co^{II}-substituted enzyme revealed a six-coordinate site (protein alone or with αKG) that became five-coordinate upon taurine addition. The Co^{II} spectrum was not perturbed by a series of anions or oxidants, suggesting the Co^{II} is inaccessible and could be used to stabilize the protein. NOG competed weakly ($K_i \sim 290$ μM) with αKG for binding to TauD, with the increased electron density of NOG yielding electronic transitions for NOG-Fe^{II}-TauD and taurine-NOG-Fe^{II}-TauD at 380 nm (ε_{380} 90–105 M^{-1} cm^{-1}). The spectra of the NOG-bound TauD species did not change significantly upon oxygen exposure, arguing against the formation of an oxygen-bound state mimicking an early intermediate in catalysis.
© 2005 Elsevier Inc. All rights reserved.

Keywords: α-Ketoglutarate; Oxoglutarate; Ferrous; Hydroxylase; Dioxygenase; Metal-substituted; Spectroscopy; Inhibition

Fe^{II}/α-ketoglutarate (αKG)-dependent dioxygenases couple the oxidative decarboxylation of αKG to the oxidation of their primary substrates using a mononuclear, non-heme iron metallocenter [1]. These enzymes catalyze a wide variety of crucial chemical transformations including the repair of alkylation damage in DNA or RNA [2,3], sensing of hypoxia [4], modification of structural proteins [5], synthesis of various metabolites ranging from antibiotics [6] to plant hormones [7,8], and degradation of compounds such as herbicides [9] and phytanic acids [10]. The focus of this study is the archetype member of this enzyme family, *Escherichia coli* taurine/αKG dioxygenase (TauD) that metabolizes aminoethanesulfonate (Scheme 1) to produce sulfite as a cellular sulfur source [11].

Recent crystallographic and spectroscopic studies of TauD have confirmed many aspects of the general enzyme mechanism of Fe^{II}/αKG-dependent dioxygenases (Scheme 2) that was first proposed over two decades ago [12]. Structural studies [13,14] reveal that the Fe^{II} center is ligated by three amino acid side chains on the same face of the metal: His99, Asp101, and His255. In the absence of substrate, three water molecules complete the six-coordinate environment (A). Two waters are displaced upon binding of αKG (shown as $RCOCOO^-$), which coordinates the Fe^{II} center through its C-1 carboxylate and C-2 carbonyl moieties (B) producing a diagnostic metal-to-ligand charge-transfer transition with a λ_{max} at 530 nm and ε_{530} of 140–240 M^{-1} cm^{-1} [15,16]. Taurine (illustrated by R′—H) binds near the active site and promotes dissociation of the

* Corresponding author. Fax: +1 517 353 8957.
E-mail address: hausinge@msu.edu (R.P. Hausinger).

0006-291X/$ - see front matter © 2005 Elsevier Inc. All rights reserved.
doi:10.1016/j.bbrc.2005.08.223

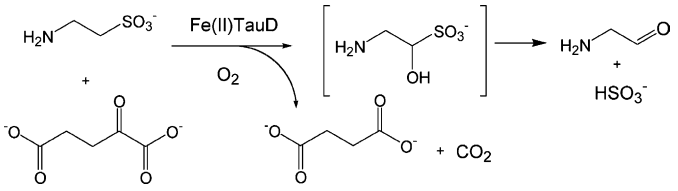

Scheme 1.

remaining water ligand to shift the λ_{max} to 520 nm with $\varepsilon_{520} = 180–270\ M^{-1}\ cm^{-1}$ [15,16], leaving the Fe^{II} five-coordinate and primed to react with oxygen (C). Binding of oxygen produces a yet uncharacterized Fe^{III}-superoxo or Fe^{IV}-peroxo species (D) that attacks the αKG carbonyl group, leading to decomposition of αKG and heterolytic O–O bond cleavage. The resulting Fe^{IV}-oxo species (E) inserts oxygen into the target C–H bond of the substrate by hydrogen atom transfer and oxygen rebound, as found in heme-type oxygenases, to restore the Fe^{II} state of the enzyme. The Fe^{IV}-oxo species has been identified on the basis of stopped-flow UV/visible spectroscopy, freeze-quench Mössbauer analyses, EPR spectroscopy of cryoreduced sample, cryogenic continuous-flow resonance Raman studies, and X-ray absorption spectroscopy [16–21].

Here, we examine the kinetics and spectroscopy of TauD interaction with three well-known inhibitors of this class of enzymes. Co^{II} and Ni^{II} inhibit prolyl and asparaginyl hydroxylases that target the hypoxia inducible factor (HIF), involved in oxygen sensing [22], so the metal ions lead to cellular gene expression changes mimicking those observed during hypoxia [23,24]. In addition, Co^{II} inhibits several other enzyme family members including TauD [11] and 1-aminocyclopropanecarboxylate oxidase, for which the Co-bound crystal structure is known [25]. Despite the importance of these inhibitory metal ions to the functioning of Fe^{II}/αKG-dependent dioxygenases, few kinetic characterization studies and no spectroscopic investigations have been reported. Similarly, the αKG analogue *N*-oxalylglycine (NOG) is an established inhibitor of procollagen prolyl 4-hydroxylase [26,27] as well as HIF-specific prolyl and asparaginyl hydroxylases [28–30]. In the asparaginyl hydroxylase known as factor inhibiting HIF (FIH), the structure of the NOG-bound enzyme was determined and NOG was found to coordinate Fe in the same manner as the αKG shown in B of Scheme 2 [31]. Furthermore, inhibition of the iron-mediated degradation of the iron regulatory protein 2 by dimethyl-NOG (which is hydrolyzed to NOG by esterases within the cell) was cited as evidence for the participation of an Fe^{II}/αKG-dependent dioxygenase in this pathway [32,33]. As with the inhibitory metals, few NOG-related studies address the kinetics of inhibition and none examine the spectroscopic properties of the inhibited enzyme. We have chosen to study these aspects of Co^{II}, Ni^{II}, and NOG interaction with TauD as a paradigm for related systems. In addition, we sought to obtain new insights into the structures and properties of the early intermediates in TauD catalysis.

Materials and methods

Purification of TauD apoprotein. Cultures of *E. coli* BL21(DE3) with pME4141 [11], containing *tauD* under the control of the T7 RNA polymerase promoter, were grown in TB medium (1 L) at 37 °C with stirring at 200 rpm. When cultures reached an A_{600} of ~0.4, *tauD* expression was induced by the addition of isopropyl-β-D-thiogalactopyranoside to a final concentration of 0.1 mM. Cells were harvested after ~12 h by centrifugation for 10 min at 10,000*g* and 4 ° C. The cell pellet was resuspended in 20 mL of 20 mM Tris with 1 mM EDTA (TE) buffer (pH 8.0). The sample was stored at −80 °C until disrupting the cells by using a French pressure apparatus. The lysate was clarified by centrifugation for 40 min at 150,000*g* and applied to a DEAE-Sepharose column (5.0 × 30 cm, Amersham Biosciences). The column was rinsed with two column volumes of TE buffer (pH 8.0) and eluted by using a linear 1500 mL gradient from 70 to 230 mM NaCl in the same buffer at a flow rate of 7 mL/min. Fractions containing TauD were concentrated in an Amicon stirred cell concentrator with a 30 kDa cutoff membrane. The concentrated eluant was loaded onto a high-performance phenyl-Sepharose column (2.5 × 30 cm, Amersham Biosciences) equilibrated with TE buffer (pH 8.0) containing 500 mM $(NH_4)_2SO_4$. Proteins were eluted with a 1200 mL linear gradient from 500 to 0 mM $(NH_4)_2SO_4$ in the same buffer at a flow rate of 5 mL/min. The TauD-containing fractions were concentrated and extensively dialyzed

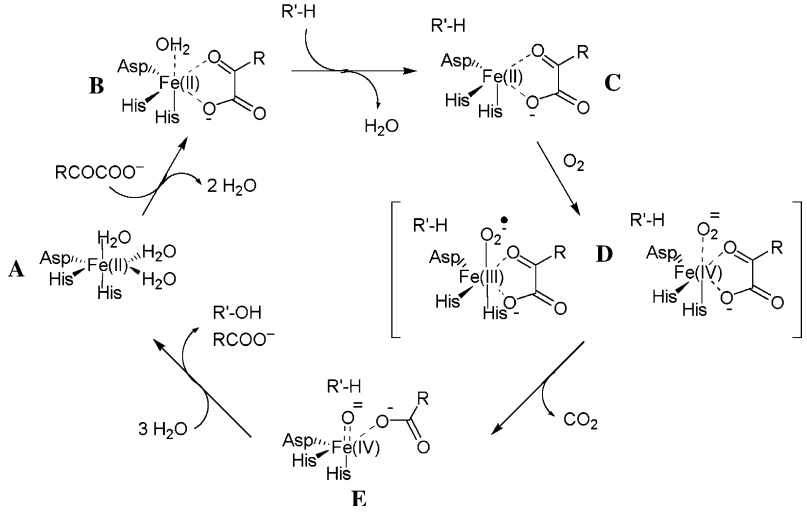

Scheme 2.

against 25 mM Tris buffer (pH 8.0) at 4 °C. Purified TauD apoprotein exhibited a single 32.2 kDa band when examined by denaturing polyacrylamide gel electrophoresis. Protein concentrations were estimated by using ε_{280} 46,400 M^{-1} cm^{-1}. The dialyzed apoprotein was stored frozen at −80 °C.

Enzyme assays. TauD activity was measured by using Ellman's reagent to quantify sulfite, as previously described [11]. One unit (U) of enzyme activity is defined as the amount of enzyme that releases 1 μmol of sulfite per minute at 30 °C in assay buffer containing 25 mM Tris (pH 8.0), 50 or 100 μM Fe^{II}, 50 or 100 μM ascorbate, 100 or 500 μM αKG, and 1 mM taurine. The TauD used in these studies had a specific activity ranging from 3 to 6.4 U (mg of protein)$^{-1}$.

Characterization of inhibition kinetics. Steady-state inhibition assays were carried out during 5 min incubations using the typical assay conditions (sometimes with one component varied in concentration) and amended with the indicated concentrations of inhibitor. The assays were initiated either by adding enzyme or by adding Fe^{II} to the assay buffers. In addition, the time dependence of inhibition was assessed in some cases by removing timed aliquots to an EDTA quench solution.

Electronic spectroscopy. Spectra were recorded at room temperature on a Shimadzu UV-2401 UV/visible spectrophotometer. All stock solutions for anaerobic binding studies were prepared inside serum vials sealed with butyl rubber stoppers and purged of oxygen by several rounds of vacuum degassing and flushing with argon using a vacuum manifold. Stock solutions of αKG (50 or 100 mM), taurine (50 or 100 mM), and NOG (100 mM) were prepared in 25 mM Tris buffer (pH 8.0). Ferrous ammonium sulfate stock solutions (25 mM) containing 5 mM ascorbate were prepared by several rounds of degassing and argon flushing of the solids, followed by addition of the desired volume of H_2O. $CoCl_2$ and $NiCl_2$ stock solutions (25 mM) were prepared by several rounds of degassing and flushing with argon inside a sealed serum vial. TauD apoprotein (0.25 or 0.5 mM subunit in 25 mM Tris buffer, pH 8.0) was placed into a 1 cm path length, 1 mL quartz cuvette fitted with a stopper and purged with argon. Other components were added by using gastight syringes (Hamilton) that had been flushed with anaerobic buffer. Selected samples were mixed with an equal volume of buffer sparged with 100% O_2, and spectral changes were monitored over time. The effect of added H_2O_2 was examined in one sample. All spectra were corrected to account for sample dilutions.

Results and discussion

Kinetics of inhibition of TauD by Co^{II} and Ni^{II}

The effects of Co^{II} and Ni^{II} on TauD activity were examined by using two methods to initiate the assays. First, TauD apoprotein was added to standard assay mixes containing Fe^{II} and varied concentrations of the inhibitory metal ions, incubated for 5 min, and the total sulfite product was measured (Fig. 1, solid lines). The data were fit to Eq. (1) (where [M] is the inhibitory metal ion concentration) to determine the IC_{50} (inhibitor concentration resulting in 50% inhibition, with the approximate range of this value shown in parentheses). The IC_{50} of Co^{II} was 41 μM (30–70 μM) while that of Ni^{II} was 32 μM (20–40 μM). When the TauD inhibition assays were repeated using Fe^{II} addition to initiate the reaction (Fig. 1, dashed lines), the observed IC_{50} values were 1.9 μM (1–3.5 μM) and 0.71 μM (0.60–1.0 μM) for Co^{II} and Ni^{II}, respectively. The large differences in IC_{50} values observed when using the distinct methods to initiate the reaction suggest that Fe^{II} does not readily displace the inhibitory metal ions previously bound to the protein. These differences also highlight the fact that steady-state assays that assume rapid equilibrium kinetics are inadequate for defining the true kinetic inhibition mechanism of metal ions. Despite this caveat, the IC_{50} values obtained for TauD were compared to those reported for three human HIF-specific prolyl 4-hydroxylase isozymes (38 ± 8, 100 ± 15, and 9 ± 4 μM for Co^{II}; 130 ± 76, >1000, and 120 ± 49 μM for Ni^{II}) and a collagen-specific prolyl 4-hydroxylase (14 ± 3 μM for Co^{II} and 37 ± 11 μM for Ni^{II}) along with the K_i values estimated for FIH inhibition (1.0 ± 0.4 μM for Co^{II} and 4 ± 1 μM for Ni^{II}) [22]. Curiously, Co^{II} and Ni^{II} inhibition of the HIF prolyl 4-hydroxylases was incomplete with up to 50% activity remaining at 0.5 mM Co^{II} and up to 55% activity remaining at 1 mM Ni^{II}. We attribute the incomplete inhibition of the prolyl 4-hydroxylases to their purification as partial holoproteins, compared to TauD that was purified as the apoprotein.

$$\%\ \text{activity remaining} = 100 - 100[\text{M}]/(\text{IC}_{50} + [\text{M}]). \quad (1)$$

To better define the kinetic mechanism of inhibition by metal ions, the time-dependence of Co^{II} and Ni^{II} inhibition was determined (Figs. 2A and B). In the absence of inhibitory metal ion, sulfite production began immediately (i.e., TauD apoprotein binds Fe^{II} rapidly) and increased steadily. When

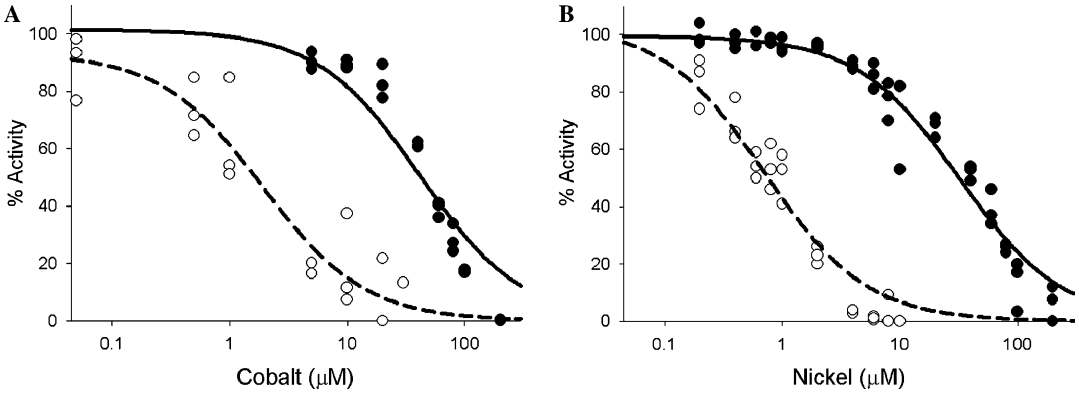

Fig. 1. Inhibition of TauD by Co^{II} and Ni^{II}. The concentrations of sulfite produced during 5 min incubations were used to assess the percent activity of TauD in standard assay conditions containing the indicated concentrations of Co^{II} (A) and Ni^{II} (B). The solid circles represent data associated with assays initiated with TauD apoprotein, whereas the open circles represent data for assays initiated by Fe^{II} addition to samples exposed to inhibitory metal ions for 2 min. The data were fit to Eq. (1) to calculate IC_{50} values.

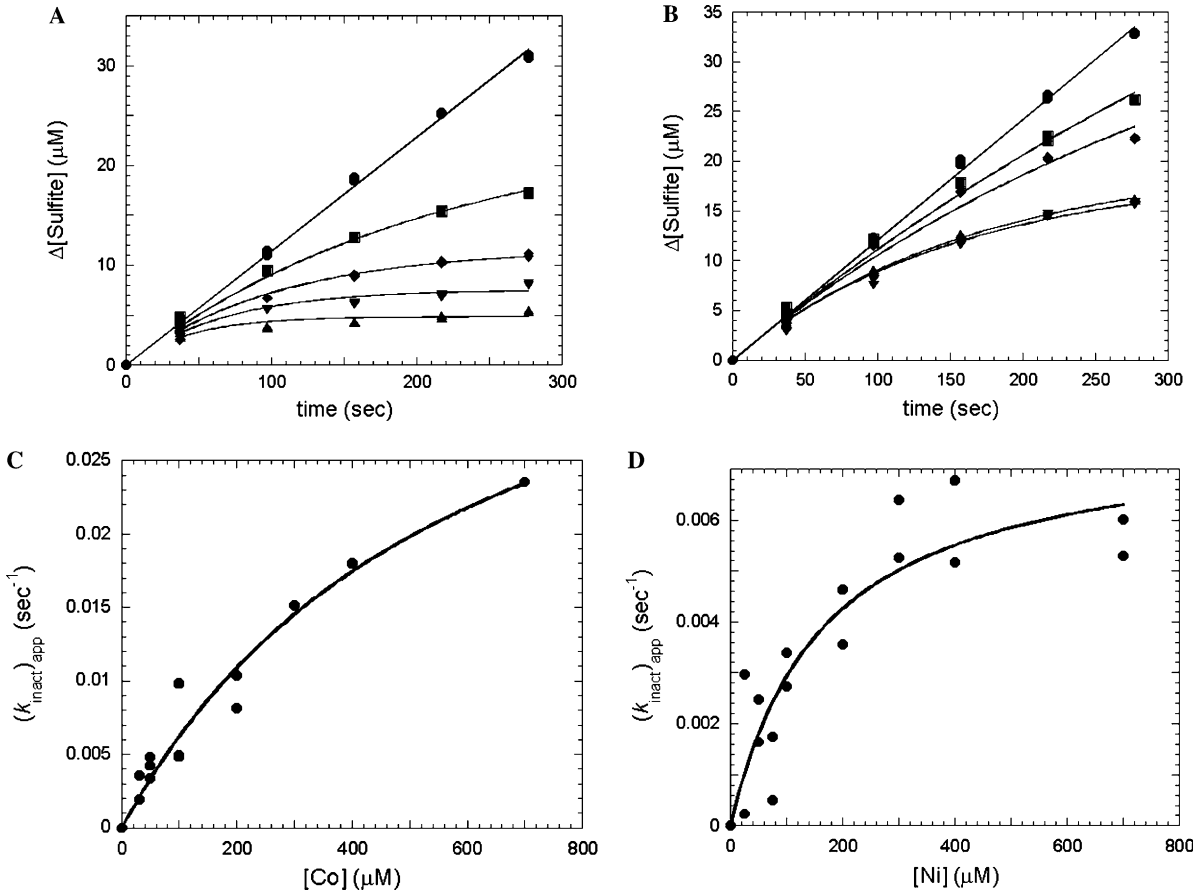

Fig. 2. Time-dependent inhibition of TauD by Co^{II} and Ni^{II}. TauD apoprotein was added to standard assay conditions and varied concentrations of Co^{II} or Ni^{II} (including 0 μM, ●; 50 μM, ■, 100 μM, ♦; 300 μM, ▼, and 700 μM, ▲) were added after 23 s (equivalent to the zero time point in the subset of studies illustrated in (A,B)). Subsequent productions of sulfite were analyzed according to Eq. (2) to determine the effects of inhibitory metal concentrations on k_{inact}, the apparent rates of inactivation, as illustrated in (C,D).

various concentrations of Co^{II} or Ni^{II} were added at 23 s into the assays, the rates of sulfite production were observed to decrease over time. The apparent first-order rate constants of enzyme inactivation were calculated for each assay according to Eq. (2) (where P_t is the amount of product at time t, v_i is the initial rate, and k_{inact} is the apparent inactivation rate constant), and the values were replotted as a function of inhibitory metal ion concentrations (Figs. 2C and D). The apparent k_{inact} values were observed to saturate at high concentrations of metal ions, consistent with slow-binding inhibition kinetics (Scheme 3) [34]. The initial dissociation constant $K_i(k_{-1}/k_1)$ was estimated to be 600 ± 180 μM for Co^{II} and 166 ± 65 μM for Ni^{II}, and k_3 (equivalent to $(k_{inact})_{max}$) was estimated as 0.044 ± 0.008 s^{-1} for Co^{II} and 0.078 ± 0.0012 s^{-1} for Ni^{II}.

$$P_t = v_i(1 - \exp(-k_{inact}t))/k_{inact}. \quad (2)$$

$$E + I \underset{k_{-1}}{\overset{k_1}{\rightleftharpoons}} EI \underset{k_{-2}}{\overset{k_2}{\rightleftharpoons}} EI^*$$

Scheme 3.

Spectroscopy of Co^{II} and Ni^{II} interaction with TauD

The addition of Co^{II} to an anaerobic sample of TauD (Fig. 3A) resulted in formation of a broad peak between 450 and 600 nm, with λ_{max} at 530 nm and ε_{530} of 70 M^{-1} cm^{-1} (calculated on the basis of the difference spectrum of Co^{II}-TauD minus TauD). The addition of αKG had little effect on the spectrum, whereas the further addition of taurine resulted in features at 565, 552, and 500 nm with extinction coefficients of 204, 200, and 127 M^{-1} cm^{-1} (calculated on the basis of the difference spectrum for taurine-αKG-Co^{II}-TauD minus TauD). The magnitude of the Co^{II} extinction coefficient has been shown empirically to correlate with the coordination number in Co^{II} proteins: six-coordinate sites have extinction coefficients of about 50 M^{-1} cm^{-1}, five-coordinate sites have values between 50 and 300 M^{-1} cm^{-1}, and four-coordinate sites possess a coefficient of more than 300 M^{-1} cm^{-1} [35]. We conclude that the Co^{II} sites in Co^{II}-TauD and αKG-Co^{II}-TauD are six-coordinate, whereas that in taurine-αKG-Co^{II}-TauD is five-coordinate. Thus, the binding of substrate most likely leads to dissociation of a water molecule in this metal-substituted protein just as in the active, Fe^{II}-containing enzyme.

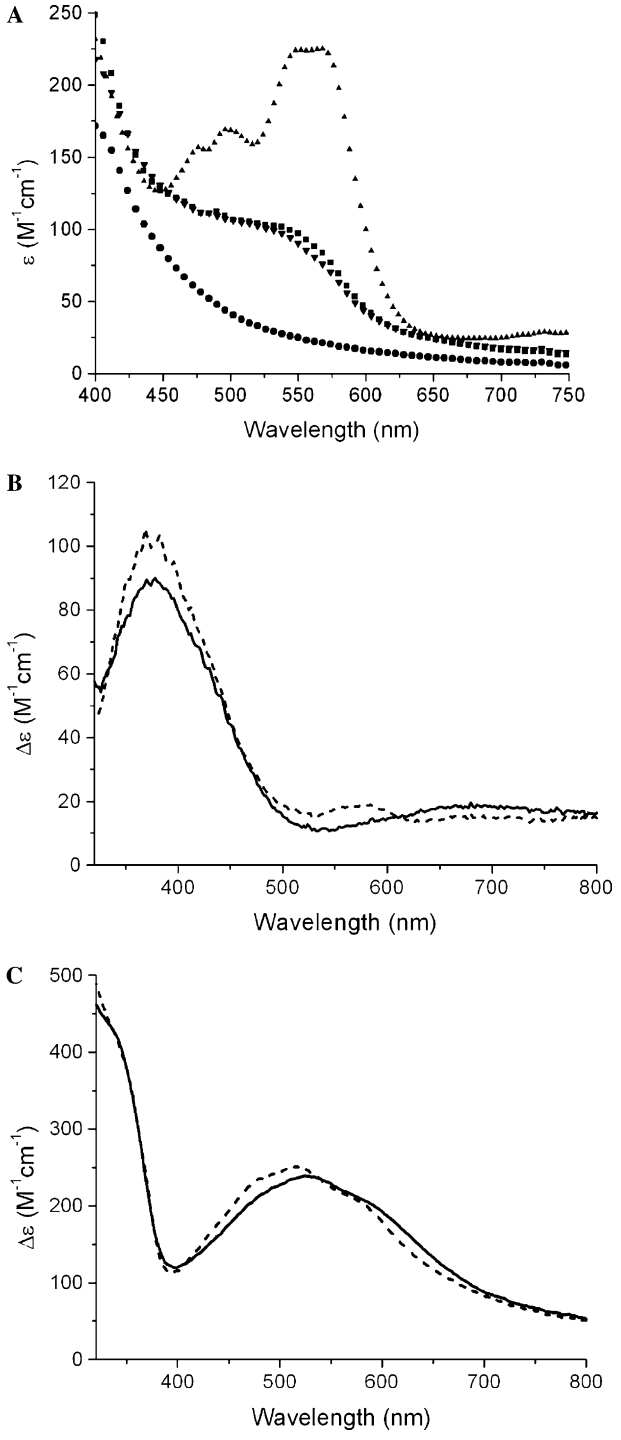

Fig. 3. Electronic spectra of Co^{II}-substituted, NOG-Fe^{II}, and αKG-Fe^{II} forms of TauD. (A) An anaerobic solution of TauD apoprotein (550 μM subunit, circles) was adjusted to contain near stoichiometric amounts of Co^{II} (inverted triangles), 2 mM αKG (squares), and 2 mM taurine (triangles) in 25 mM Tris buffer, pH 8.0. (B) Analogous spectra were collected for 250 μM TauD while substituting Fe^{II} for Co^{II} and 10 mM NOG for αKG, with difference spectra shown for the taurine-NOG-Fe^{II}-TauD minus Fe^{II}-TauD (dashed line) and the NOG-Fe^{II}-TauD minus Fe^{II}-TauD samples (solid line). (C) Analogous spectra were collected using Fe^{II} and αKG, again showing difference spectra for the taurine-αKG-Fe^{II}-TauD minus Fe^{II}-TauD (dashed line) and the αKG-Fe^{II}-TauD minus Fe^{II}-TauD (solid line) samples.

We examined the accessibility of TauD-bound Co to exogenous ligands using both taurine-αKG-Co^{II}-TauD and αKG-Co^{II}-TauD. No spectral changes were detected for either species upon addition of CN^-, OCN^-, SCN^-, or ClO^- at 4 mM concentrations, or in the presence of 200 mM NaCl. Although the metal coordination environment of taurine-αKG-Co^{II}-TauD appears to closely resemble that of taurine-αKG-Fe^{II}-TauD, the spectrum of the Co^{II}-containing species remained unchanged when exposed to oxygen. Furthermore, despite precedence for the transformation of Co^{II} species to Co^{III}-OOH model compounds [36,37], no spectral perturbations were observed when H_2O_2 (up to 750 μM) was added to taurine-αKG-Co^{II}-TauD.

In contrast to the situation for Co^{II}, the addition of Ni^{II} did not affect the spectra of TauD, protein plus αKG, protein with both substrates, or for these components plus oxygen (data not shown).

Kinetics of Inhibition of TauD by NOG

Steady-state kinetic inhibition studies (data not shown) were used to establish that NOG competed with αKG for binding to TauD, with a K_i of 290 ± 90 μM. *N*-Oxalylglycine should be able to form all of the ionic interactions of αKG and it contains an oxamic acid moiety as a potentially better bidentate ligand for the enzyme-bound Fe^{II}, so we were surprised by the weak inhibition of TauD by this compound. For comparison, NOG was shown to be a competitive inhibitor of collagen prolyl 4-hydroxylase and FIH with markedly different K_i values of 1.9–7.0 μM [26] and 1.2 ± 0.3 mM [30]. The reasons for this wide range of K_i values for these enzymes remain unclear, but interactions with the protein side chains probably play a role in determining this value. Studies with the structurally related compound *N*-oxalyl-D-phenylalanine provided a K_i of 83 ± 18 μM for FIH,14-fold smaller than that of NOG [30].

Spectroscopy of NOG interaction with TauD

The spectra of NOG-Fe^{II}-TauD and taurine-NOG-Fe^{II}-TauD (Fig. 3B) differ significantly from the previously described spectra of αKG-Fe^{II}-TauD and taurine-αKG-Fe^{II}-TauD (shown for comparison in Fig. 3C). We interpret this result in terms of the excess electron density of NOG compared to αKG (note the trianionic form of NOG versus the

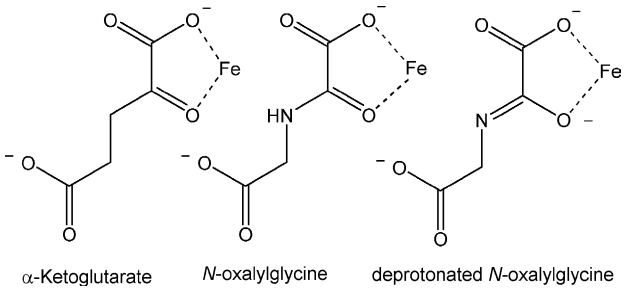

Scheme 4.

dianionic αKG, Scheme 4) which causes a shift of the metal-to-ligand charge-transfer transition to higher energy. While αKG-Fe^{II}-TauD is known to react with oxygen resulting in αKG decomposition, protein self-hydroxylation, and the generation of a 550 nm chromophore [38], the spectra of NOG-Fe^{II}-TauD and taurine-NOG-Fe^{II}-TauD did not change at a significant rate upon exposure to oxygen. The reduced O_2 reactivity for these species also contrasts with that observed for the product complex (succinate-Fe^{II}-TauD) that generates a 720 nm chromophore when exposed to O_2 [39]. The αKG- and succinate-derived ligand-to-metal charge-transfer transitions arise from chelation of Fe^{III} by the catecholate produced by hydroxylation of Tyr73, with or without bound bicarbonate ligand [39]. We conclude that hydroxylation of Tyr73 is greatly reduced using NOG-Fe^{II}-TauD and that NOG does not undergo oxidative decarboxylation.

Conclusions

Steady-state kinetic approaches are inappropriate for determining the kinetics of inhibition of Fe^{II}/αKG-dependent hydroxylases by metal ions; rather, slow-binding kinetic inhibition methods must be utilized. The chromophore generated upon binding of both substrates to Co^{II}-substituted protein might serve as a useful diagnostic marker for this enzyme family. While the resulting Co^{II} center is most likely five-coordinate in TauD, it does not react with added ligands including oxidants. The low reactivity of the Co^{II}- and Ni^{II}-substituted enzymes could be exploited during purification and crystallization efforts to stabilize related proteins against self-hydroxylation reactions. Despite the close structural similarity of NOG to αKG, this is a weak competitive inhibitor of TauD and the K_i ranges widely for different enzymes. The NOG-bound state of the enzyme does not react with oxygen to catalyze oxidative decarboxylation.

Acknowledgments

We thank Dr. Nicolai Burzlaff for providing NOG. These studies were supported by the National Institutes of Health (GM063584 to R.P.H.).

References

[1] R.P. Hausinger, Fe(II)/α-ketoglutarate-dependent hydroxylases and related enzymes, Crit. Rev. Biochem. Mol. Biol. 39 (2004) 21–68.
[2] S.C. Trewick, T.F. Henshaw, R.P. Hausinger, T. Lindahl, B. Sedgwick, Oxidative demethylation by *Escherichia coli* AlkB directly reverts DNA base damage, Nature 419 (2002) 174–178.
[3] P.A. Aas, M. Otterlei, P.O. Falnes, C.B. Vagbe, F. Skorpen, M. Akbari, O. Sundheim, M. Bjoras, G. Slupphaug, E. Seeberg, H.E. Krokan, Human and bacterial oxidative demethylases repair alkylation damage in both RNA and DNA, Nature 421 (2003) 859–863.
[4] C.J. Schofield, P.J. Radcliffe, Oxygen sensing by hydroxylases, Nat. Rev. Mol. Cell Biol. 5 (2004) 343–354.
[5] K.I. Kivirikko, T. Pihlajaniemi, Collagen hydroxylases and the protein disulfide isomerase subunit of prolyl 4-hydroxylase, Adv. Enzymol. Rel. Areas Mol. Biol. 72 (1998) 325–398.
[6] J.E. Baldwin, E. Abraham, The biosynthesis of penicillins and cephalosporins, Nat. Prod. Rep. 5 (1988) 129–145.
[7] R.A. Dixon, C.L. Steele, Flavonoids and isoflavonoids—a gold mine for metabolic engineering, Trend Plant Sci. 4 (1999) 394–400.
[8] P. Hedden, Recent advances in gibberellin biosynthesis, J. Exp. Bot. 50 (1999) 553–563.
[9] F. Fukumori, R.P. Hausinger, Purification and characterization of 2,4-dichlorophenoxyacetate/α-ketoglutarate dioxygenase, J. Biol. Chem. 268 (1993) 24311–24317.
[10] M. Mukherji, C.J. Schofield, A.S. Wierzbicki, G.A. Jansen, R.J.A. Wanders, M.D. Lloyd, The chemical biology of branched-chain lipid metabolism, Prog. Lipid Res. 42 (2003) 359–376.
[11] E. Eichhorn, J.R. van der Ploeg, M.A. Kertesz, T. Leisinger, Characterization of α-ketoglutarate-dependent taurine dioxygenase from *Escherichia coli*, J. Biol. Chem. 272 (1997) 23031–23036.
[12] H.M. Hanauske-Abel, V. Günzler, A stereochemical concept for the catalytic mechanism of prolylhydroxylase. Applicability to classification and design of inhibitors, J. Theor. Biol. 94 (1982) 421–455.
[13] J.M. Elkins, M.J. Ryle, I.J. Clifton, J.C. Dunning Hotopp, J.S. Lloyd, N.I. Burzlaff, J.E. Baldwin, R.P. Hausinger, P.L. Roach, X-ray crystal structure of *Escherichia coli* taurine/α-ketoglutarate dioxygenase complexed to ferrous iron and substrates, Biochemistry 41 (2002) 5185–5192.
[14] J.R. O'Brien, D.J. Schuller, V.S. Yang, B.D. Dillard, W.N. Lanzilotta, Substrate-induced conformational changes in *Escherichia coli* taurine/α-ketoglutarate dioxygenase and insight into the oligomeric structure, Biochemistry 42 (2003) 5547–5554.
[15] M.J. Ryle, R. Padmakumar, R.P. Hausinger, Stopped-flow kinetic analysis of *Escherichia coli* taurine/α-ketoglutarate dioxygenase: interactions with α-ketoglutarate, taurine, and oxygen, Biochemistry 38 (1999) 15278–15286.
[16] P.K. Grzyska, M.J. Ryle, G.R. Monterosso, J. Liu, D.P. Ballou, R.P. Hausinger, Steady-state and transient kinetic analyses of taurine/α-ketoglutarate dioxygenase: effects of oxygen concentration, alternative sulfonates, and active site variants on the Fe(IV) intermediate, Biochemistry 44 (2005) 3845–3855.
[17] J.C. Price, E.W. Barr, T.E. Glass, C. Krebs, J.M. Bollinger Jr., Evidence for hydrogen abstraction from C1 of taurine by the high-spin Fe(IV) intermediate detected during oxygen activation by taurine:α-ketoglutarate dioxygenase (TauD), J. Am. Chem. Soc. 125 (2003) 13008–13009.
[18] J.C. Price, E.W. Barr, B. Tirupati, J.M. Bollinger Jr., C. Krebs, The first direct characterization of a high-valent iron intermediate in the reaction of an α-ketoglutarate-dependent dioxygenase: a high-spin Fe(IV) complex in taurine/α-ketoglutarate dioxygenase (TauD) from *Escherichia coli*, Biochemistry 42 (2003) 7497–7508.
[19] J.C. Price, E.W. Barr, L.M. Hoffart, C. Krebs, J.M. Bollinger Jr., Kinetic dissection of the catalytic mechanism of taurine:α-ketoglutarate dioxygenase (TauD) from *Escherichia coli*, Biochemistry 44 (2005) 8138–8147.
[20] D.A. Proshlyakov, T.F. Henshaw, G.R. Monterosso, M.J. Ryle, R.P. Hausinger, Direct detection of oxygen intermediates in the non-heme Fe enzyme taurine/α-ketoglutarate dioxygenase, J. Am. Chem. Soc. 126 (2004) 1022–1023.
[21] P.J. Riggs-Gelasco, J.C. Price, R.B. Guyer, J.H. Brehm, E.W. Barr, J.M. Bollinger Jr., C. Krebs, EXAFS spectroscopic evidence for an Fe=O unit in the Fe(IV) intermediate observed during oxygen activation by taurine: α-ketoglutarate dioxygenase, J. Am. Chem. Soc. 126 (2004) 8108–8109.
[22] M. Hirsilä, P. Koivunen, L. Xu, T. Seeley, K.I. Kivirikko, J. Myllyharju, Effect of desferrioxamine and metals on the hydroxylases in the oxygen sensing pathway, FASEB J. 19 (2005) 1308–1310.
[23] M.A. Goldberg, S.P. Dunning, H.F. Bunn, Regulation of the erythropoietin gene: evidence that the oxygen sensor is a heme protein, Science 242 (1988) 1412–1415.
[24] A. Vengellur, J.M. Phillips, J.B. Hogenesch, J.J. LaPres, Gene expression profiling of hypoxia signaling in human hepatocellular carcinoma cells, Physiol. Genomics 22 (2005) 308–318.

[25] Z. Zhang, J.-S. Ren, I.J. Clifton, C.J. Schofield, Crystal structure and mechanistic implications of 1-aminocyclopropane-1-carboxylic acid oxidase—the ethylene-forming enzyme, Chem. Biol. 11 (2004) 1383–1394.
[26] E. Baader, G. Tschank, K.H. Baringhaus, H. Burghard, V. Gunzler, Inhibition of prolyl 4-hydroxylase by oxalyl amino acid derivatives in vitro, in isolated microsomes and in embryonic chicken tissues, Biochem. J. 300 (1994) 525–530.
[27] C.J. Cunliffe, T.J. Franklin, N.J. Hales, G.B. Hill, Novel inhibitors of prolyl 4-hydroxylase. 3. Inhibition by the substrate analogue N-oxaloglycine and its derivatives, J. Med. Chem. 35 (1992) 2652–2658.
[28] D.A. Chan, P.D. Sutphin, N.C. Denko, A.J. Giaccia, Role of prolyl hydroxylation in oncogenically stabilized hypoxia-inducible factor-1 α, J. Biol. Chem. 277 (2002) 40112–40117.
[29] P. Wojtaszek, C.G. Smith, G.P. Bolwell, Ultrastructural localization and further biochemical characterization of prolyl 4-hydroxylase from *Phaseolus vulgaris*: comparative analysis, Int. J. Cell Biol. 31 (1999) 463–477.
[30] M.A. McDonough, L.A. McNeill, M. Tilliet, C.A. Papmichaël, Q.-Y. Chen, B. Banerji, K.S. Hewitson, C.J. Schofield, Selective inhibition of factor inhibiting hypoxia-inducible factor, J. Am. Chem. Soc. 127 (2005) 7680–7681.
[31] J.M. Elkins, K.S. Hewitson, L.A. McNeill, J.F. Seibel, I. Schlemminger, C.W. Pugh, P.J. Ratcliffe, C.J. Schofield, Structure of factor-inhibiting hypoxia-inducible factor (HIF) reveals mechanism of oxidative modification of HIF-1α, J. Biol. Chem. 278 (2003) 1802–1806.
[32] J. Wang, G. Chen, M. Muckenthaler, B. Galy, M.W. Hentze, K. Pantopoulos, Iron-mediated degradation of IRP2, an unexpected pathway involving a 2-oxoglutarate-dependent oxygenase activity, Mol. Cell. Biol. 24 (2004) 954–965.
[33] E.S. Hanson, M.L. Rawlins, E.A. Leibold, Oxygen and iron regulation of iron regulatory protein 2, J. Biol. Chem. 278 (2003) 40337–40342.
[34] J.F. Morrison, C.T. Walsh, The behavior and significance of slow-binding enzyme inhibitors, Adv. Enzymol. Rel. Areas Mol. Biol. 61 (1988) 201–301.
[35] I. Bertini, C. Luchinat, Secondary High spin cobalt(II) as a probe for the investigation of metalloproteins, in: G.L. Eichhorn, L.G. Marzilli (Eds.), Advances in Inorganic Biochemistry, Elsevier Science Publishing Company, New York, NY, 1984, pp. 71–111.
[36] C. Rajani, J.R. Kincaid, D.H. Petering, Resonance Raman studies of HOO-Co(III)bleomycin and Co(III)bleomycin: identification of two important vibrational modes, nu(Co–OOH) and nu(O–OH), J. Am. Chem. Soc. 126 (2004) 3829–3836.
[37] F.A. Chaves, P.K. Mascharak, Co(III)-alkylperoxo complexes: syntheses, structure-reactivity correlations, and use in the oxidation of hydrocarbons, Acc. Chem. Res. 33 (1999) 539–545.
[38] M.J. Ryle, A. Liu, R.B. Muthukumaran, R.Y.N. Ho, K.D. Koehntop, J. McCracken, L. Que Jr., R.P. Hausinger, O_2- and α-ketoglutarate-dependent tyrosyl radical formation in TauD, an α-keto acid-dependent non-heme iron dioxygenase, Biochemistry 42 (2003) 1854–1862.
[39] M.J. Ryle, K.D. Koehntop, A. Liu, L. Que Jr., R.P. Hausinger, Interconversion of two oxidized forms of TauD, a non-heme iron hydroxylase: evidence for bicarbonate binding, Proc. Natl. Acad. Sci. USA 100 (2003) 3790–3795.